The Canadian Mineralogist
Vol. 47, pp. 1423-1440 (2009)
DOI: 10.3749/canmin.47.6.1423

STRUCTURE, PETROLOGY, GEOCHEMISTRY AND ZIRCON U/Pb AND Pb/Pb GEOCHRONOLOGY OF THE SYNKINEMATIC ARCHEAN (2.7 Ga) A-TYPE GRANITES FROM THE CARAJÁS METALLOGENIC PROVINCE, NORTHERN BRAZIL

CARLOS EDUARDO DE MESQUITA BARROS

Universidade Federal do Paraná, Departamento de Geologia, Centro Politécnico, Jardim das Américas, B.P. 19001, CEP 81531-990, Curitiba, Brazil

ALEX SOUZA SARDINHA

Universidade Federal do Pará, Centro de Geociências, B.P. 8608, CEP 66075-110, Belém, Brazil

JAIME DOS PASSOS DE OLIVEIRA BARBOSA

Companhia de Pesquisa de Recursos Minerais. Av. Dr. Freitas, 3645, CEP 66095-111, Belém, Brazil

MOACIR JOSÉ BUENANO MACAMBIRA

Universidade Federal do Pará, Centro de Geociências, B.P. 8608, CEP 66075-110, Belém, Brazil

PIERRE BARBEY

CRPG–CNRS, Nancy-Université, BP 20, F–54501 Vandoeuvre-lès-Nancy, Cedex, France

ANNE-MARIE BOULLIER

LGIT, Université Joseph Fourier, BP 53, F–38041 Grenoble, Cedex, France

ABSTRACT

The Archean geological evolution of the Carajás metallogenic province is marked by A-type granite emplacement coevally with a regional shortening episode at 2.7 Ga. These A-type granites intruded metavolcano-sedimentary series of the Itacaiúnas Supergroup. We studied three massifs: Igarapé Gelado, Estrela and Serra do Rabo. The granites present low Al_2O_3 values, high $FeO_t/(FeO_t + MgO)$ and $(K_2O + Na_2O)/CaO$ values, along with high contents of Zr, Y, Nb and rare-earth elements. The Sm–Nd model ages (2.97 Ga to 3.2 Ga) and the slightly negative $\varepsilon_{Nd(t)}$ values (–0.38 to –2.06), obtained in the Estrela granite complex suggest that the magmas were most probably produced by partial melting of *ca*. 3.0 Ga rocks. Coexistence of ilmenite, ferropargasite, hastingsite and hedenbergite suggest crystallization of high-temperature melts under low fugacity of oxygen. The granites induced high-temperature ductile deformation in the contact aureole. The structural patterns of the granites suggest that their emplacement and deformation result from a continuous evolution under decreasing temperature due to the interference between inflation and horizontal shortening. The A-type granites, when first discriminated, were considered to be restricted to anorogenic or rift-related environments. Our data corroborate the fact that A-type granites can abridge a wide family of rocks formed in several tectonic regimes. The characteristics of the Carajás A-type granites point to an orogenic history considered to be related to an environment of magmatic arc.

Keywords: Archean, A-type granite, geochronology, Amazonian craton, Carajás Province, Brazil.

E-mail address: cadubarros@ufpr.br

Sommaire

L'évolution de la province métallogénique de Carajás au cours de l'Archéen est marquée par la mise en place de granites de type A contemporaine d'un épisode de raccourcissement régional datée à 2.7 Ga. Ces granites ont été mis en place dans les formations métavolcanosédimentaires du supergroupe de Itacaiúnas. Nous avons étudié trois massifs: Igarapé Gelado, Estrela et Serra do Rabo. Les roches présentent de faibles teneurs en Al_2O_3, mais des rapports $FeO_t/(FeO_t + MgO)$ et $(K_2O + Na_2O)/CaO$ et des teneurs en Zr, Y, Nb et terres rares élevées. D'après les âges modèles (2.97 Ga à 3.2 Ga) et les valeurs de $\varepsilon_{Nd(t)}$ légèrement négatives (–0.38 to –2.06) obtenus sur le complexe granitique de Estrela, les magmas pourraient dériver de la fusion partielle de roches datant de 3.0 Ga. La coexistence des minéraux comme ilménite, ferropargasite, hastingsite et hédenbergite suggère la cristallisation de liquides de haute température sous des conditions de basse fugacité d'oxygène. Les granites ont induit une déformation ductile de haute température dans les roches de l'auréole de contact. D'après les caractéristiques structurales, la mise en place des granites résulterait d'une évolution continue à température décroissante liée à l'interférence entre l'expansion des plutons et un raccourcissement horizontal régional. Les granites de type A, lorsqu'ils ont été définis, ont été considérés comme liés aux environnements anorogéniques ou de rift. Nos données montrent que ces granites peuvent englober une large famille de roches formées dans des régimes tectoniques variés. Les caractéristiques des granite A de Carajás indiqueraient une évolution orogénique possiblement liée à un environnement de type arc.

Mots-clés: Archéen, granites de type A, géochronologie, craton amazonien, province de Carajás, Brésil.

Introduction

The A-type granites were first described by Loiselle & Wones (1979) as alkaline rocks formed in anorogenic or rift-related environments and displaying low Al_2O_3 and CaO values, high incompatible element contents, along with high $FeO/(FeO + MgO)$ and K_2O/Na_2O. Since then, many authors have discussed chemical parameters for discrimination (Pearce *et al.* 1984, Whalen *et al.* 1987, Sylvester 1989, 1994), subtypes (Eby 1992, Sylvester 1994), conditions of genesis and crystallization (Giret *et al.* 1980, Anderson & Bender 1989, Clemens *et al.* 1986, Creaser *et al.* 1991, Anderson & Smith 1995) and economical potential (Haapala 1995, Costi *et al.* 2002, Bettencourt *et al.* 2005). Amongst the different petrogenetic models proposed in the last two decades, those involving either partial melting of crustal sources (Landenberger & Collins 1996, Skjerlie & Johnston 1993, Patiño-Douce 1997), preceded by a metasomatic overprint (Martin 2006), or extensive fractionation of mantle-derived magmas (Turner *et al.* 1992, Whalen *et al.* 1996) have been the most widely accepted. Martin (2006) also considered that epizonal peraluminous A-type granites could result from degassing of the magmas upon emplacement in extensional regimes. A recent review volume edited by O.T. Rämö (2005) presents the state of the art on A-type granites. Not less outstanding are the discussions on structures developed during emplacement, cooling and crystallization of granitic magmas (*e.g.,* Arzi 1978, Brun & Pons 1981, Miller & Paterson 1994, Vigneresse *et al.* 1996, Vigneresse & Clemens 2000, Pawley & Collins 2002, Vigneresse 2004). In the specific case of A-type granites, their "anorogenic" character has been questioned, studies having shown that some were emplaced in "orogenic" geodynamic contexts (*e.g.,* Pons *et al.* 1995, Liverton 1999, Thompson & Barnes 1999).

Owing to the occurrence of a large number of ore deposits, the Carajás metallogenic province in northern Brazil is considered as one of the most important mineral provinces in the world. Its tectonothermal evolution during the Archean times is associated with the emplacement of unusual A-type granites concomitantly with regional horizontal shortening. In this paper, we present a review of the structural, petrological, geochemical and geochronological characteristics of Archean A-type synkinematic granites of the Carajás province. The review is based on both published and unpublished studies of three main granite massifs located in the northern part of the Carajás region: the Estrela Granite Complex (Barros *et al.* 1997, 2001), the Serra do Rabo granite plutons (Huhn *et al.* 1999, Sardinha *et al.* 2006) and the Igarapé Gelado pluton (Barbosa 2004). In this paper, we present some examples of synkinematic A-type granites and discuss their role in the Archean evolution of the Carajás region. The aim of this work is also to improve the level of knowledge about the A-type granites through time. Considering the Archean age of the massifs studied and the relatively complex structural evolution of the Carajás metallogenic province, it is surprising that one has the possibility of describing several primary structural and petrographical features of the granitic rocks and also in their host rocks.

Geological Setting

The Carajás metallogenic province (Fig. 1), located in the southeastern part of the Amazon craton (Almeida *et al.* 1981), hosts several Au, Cu, Fe, PGE, Ni and Mn deposits (Docegeo 1988). This area represents an Archean nucleus limited to the north by the Paleoproterozoic Maroni–Itacaiúnas belt, to the east by the Neoproterozoic Araguaia fold belt, to the west by Paleoproterozoic plutonic granitic rocks and related volcanic rocks, and to the south by the Phanerozoic sedimentary cover of the Parecis Basin (Tassinari & Macambira 2004). The Carajás metallogenic province is comprised

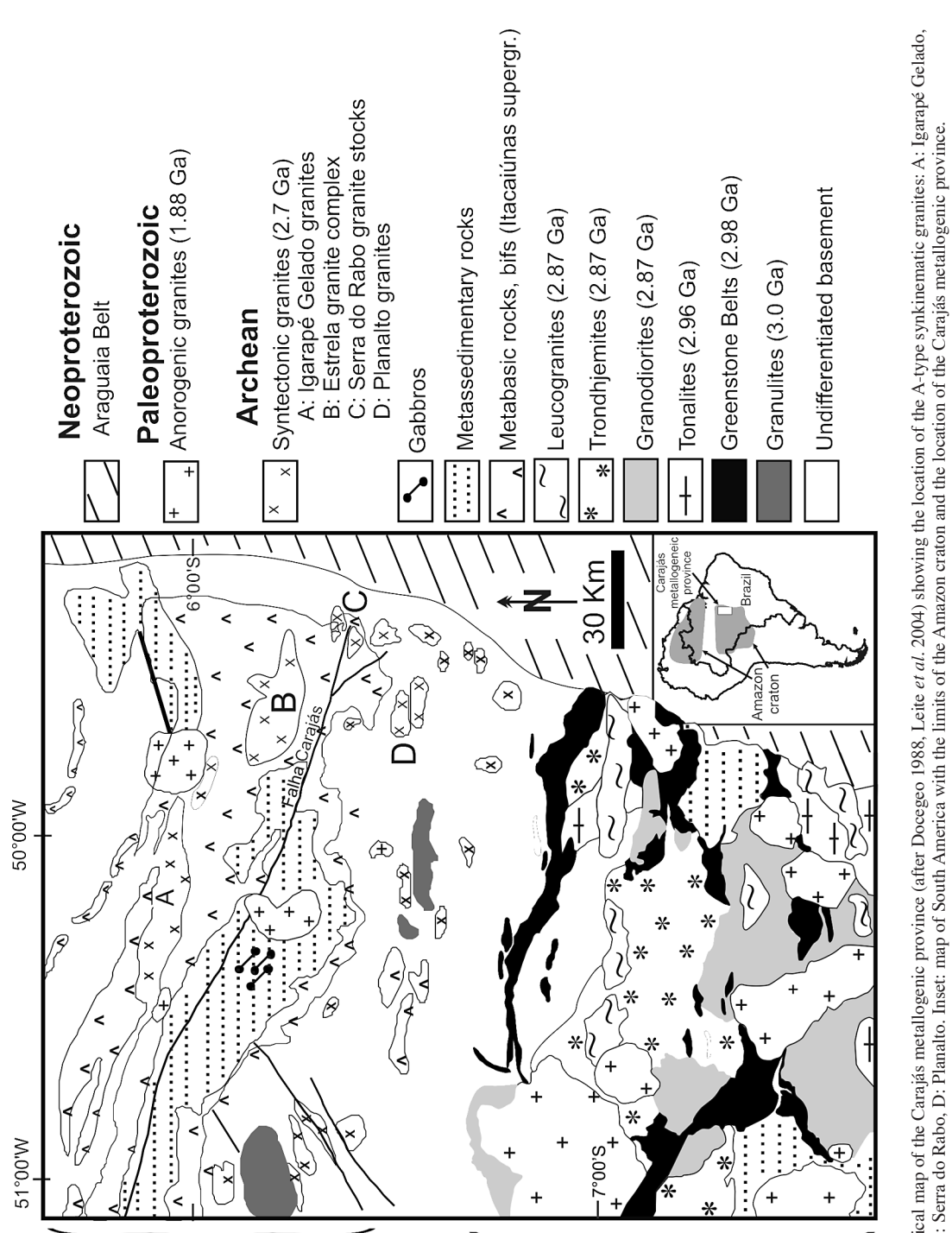

FIG. 1. Geological map of the Carajás metallogenic province (after Docegeo 1988, Leite *et al.* 2004) showing the location of the A-type synkinematic granites: A: Igarapé Gelado, B: Estrela, C: Serra do Rabo, D: Planalto. Inset: map of South America with the limits of the Amazon craton and the location of the Carajás metallogenic province.

of two domains: the Rio Maria granite–greenstone terrane to the south and the Carajás range to the north (Docegeo 1988). In the Rio Maria terrane, pillowed tholeiites dated at 2.98 Ga occurring in east–west belts are cross-cut by 2.96 Ga foliated calc-alkaline tonalites and trondhjemites, as well as by 2.87 Ga weakly foliated tonalites, trondhjemites, calc-alkaline granites and huge sanukitoid plutons such as the Rio Maria granodiorite (Dall'Agnol *et al*. 1997, Althoff *et al*. 2000, Leite *et al*. 2004). Small east–west inliers of 3.0 Ga mafic granulites have been reported to the north of the Rio Maria terrane (Pidgeon *et al*. 2000), close to the supposed limit between the two domains.

In the Carajás range, greenschist-facies metatholeiites cover large areas and present narrow layers of banded iron-formation and Mn-rich quartzites (Itacaiúnas Supergroup; Docegeo 1988). These volcanosedimentary rocks were then intruded by the 2.7 Ga Estrela, Igarapé Gelado, Serra do Rabo and Planalto synkinematic A-type granites (Fig. 2; Barros *et al*. 1997, 2001, Huhn *et al*. 1999, Barbosa 2004, Sardinha *et al*. 2006). The Carajás range corresponds to a plateau underlain by Archean sandstones and siltstones (Docegeo 1988) that cover the metatholeiites and are themselves cross-cut by sills and dykes of hydrothermally altered Archean gabbros (Barros *et al*. 1994).

Both domains are cross-cut by several discordant 1.88 Ga A-type granites (Machado *et al*. 1991, Rämö *et al*. 2002, Dall'Agnol *et al*. 2005) and underwent several episodes of strike–slip and inverse tectonic movements from 2.8 to 1.9 Ga (Pinheiro & Holdsworth 1997).

Structures and Metamorphism of the Country Rocks

The host metavolcanosedimentary series (the Itacaiúnas Supergroup) were affected by several phases of deformation and metamorphism, predated by seawater-induced hydrothermal alteration of regional extent, under greenschist-facies conditions. Locally, primary subophitic textures are preserved in massive metabasalts showing igneous pyroxene crystals replaced by actinolite (Barros & Barbey 1998, Fig. 6). Far from the 2.7 Ga A-type granites, a non-pervasive east–west foliation occurs in the metavolcanosedimentary series. In the contact aureoles around the granite bodies, deformation and recrystallization in the hornblende hornfels facies led to widespread foliated amphibolites that show a steep-plunging mineral lineation (Figs. 2, 3a) outlined by the preferred orientation of annite, plagioclase and amphibole. The aureoles are wider around the larger granitic bodies (Estrela and Igarapé Gelado). Close to the southern contact with the Estrela granite complex, metabasic rocks can locally show synkinematic porphyroblasts of garnet (Fig. 3b), indicating inverse southward movement. This movement is interpreted as a response to local stress induced by the interference between pluton emplacement and regional horizontal shortening (Barros *et al*. 2001).

Non-foliated granoblastic xenoliths of metabasic country-rocks, recrystallized under pyroxene hornfels conditions, are common in the granites. Millimeter- to centimeter-wide amphibole-bearing veins occur in both the xenoliths and amphibolites of the inner aureole (Fig. 3c). Veining has been interpreted as a result of dehydration reactions, increasing fluid pressure and mass transfer by hydraulic fracturing. After the 2.7 Ga contact metamorphism, the country rocks were affected by at least two important phases of shearing (Pinheiro & Holdsworth 1997). Major 2.5 Ga ductile shear-zones were followed at *ca*. 1.9 Ga by an episode of brittle to brittle–ductile faulting (Carajás Fault). The latter event developed under low-temperature greenschist-facies conditions (chlorite zone), and led to the transformation of the metabasic rocks into foliated tectonites. These major fault-zones strike southward of the 2.7 Ga granites, without any evidence that the granites were affected by these later phases of shearing.

Structures of the Granites

The granite bodies were mapped by combining field work and remote sensing images. The granite bodies are of variable size and may occur as small isolated plutons (Serra do Rabo: 11 × 4.5 km for the southern pluton, 14 × 4 km for the northern one), or larger massifs (Igarapé Gelado: 62 × 14 km), or as aggregated plutons (Estrela: 37 × 15 km). The large-scale structural features recognizable are the pluton shape and the foliation trajectories in both the plutons and their host rocks (Fig. 2). Most of the massifs studied present an east–west elongate shape, with the exception of a small north–south-trending pluton in the Estrela granite complex. Contacts are conformable to both petrographic facies and foliation of the country rocks.

The mesoscale structures are similar in the Estrela granite complex and the Igarapé Gelado pluton. They comprise primary igneous layering (S_0), synmagmatic stress-related foliation (S_1), high-temperature mylonites and conjugate shear zones, as well as late dissolution-induced joints. In slightly strained rocks, the preferred orientation of minerals is weak to moderate, and intracrystalline deformation corresponds only to undulose extinction and subgrains in quartz. In moderately strained rocks, quartz occurs as elongate grains with more abundant subgrains and neoblasts; feldspars may exhibit undulose extinction, kink bands and partial recrystallization of their margins (mantle-and-core texture). The ferromagnesian minerals show a strong preferred orientation, with recrystallization tails aligned along the S_1 foliation. In the mylonites, feldspar porphyroclasts occur within the fine-grained mylonitic matrix. The deformation–recrystallization relationships show that deformation occurred in a continuum from above-

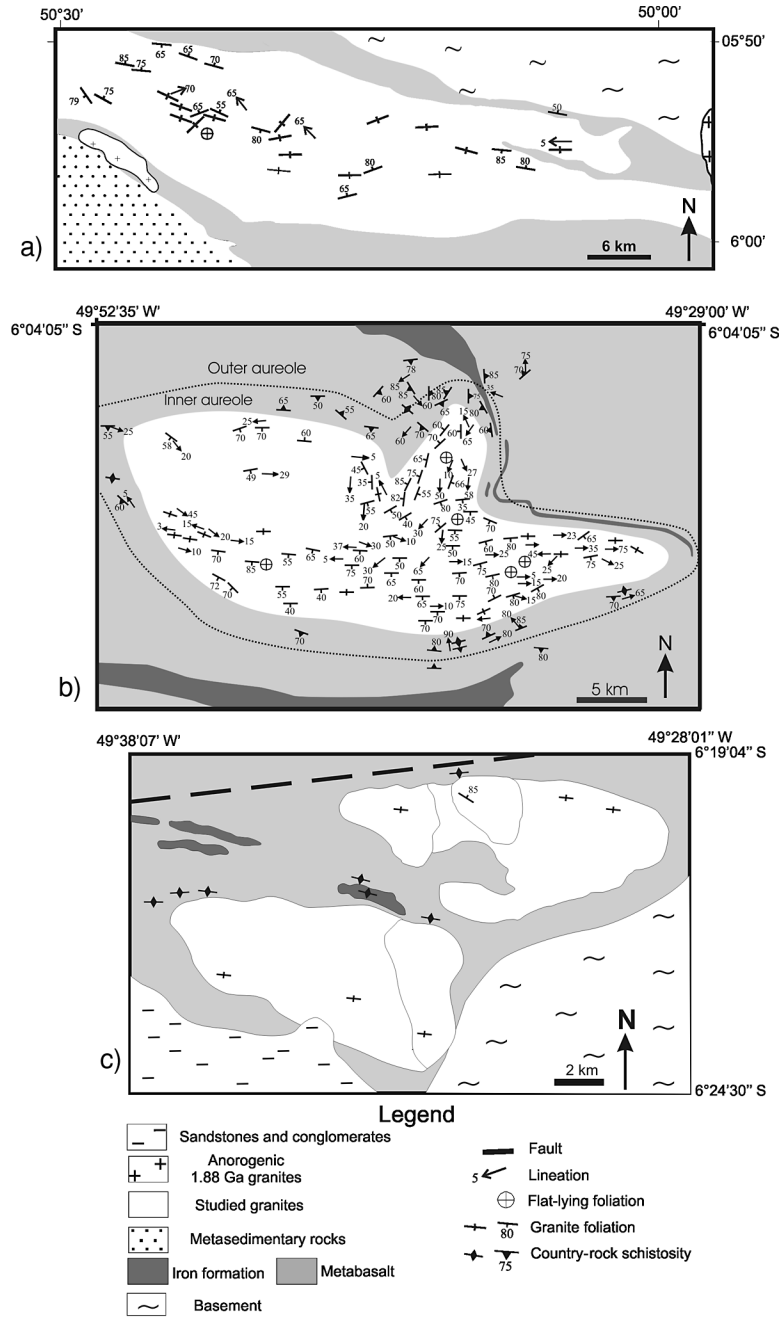

FIG. 2. Geological sketch-map of the Igarapé Gelado massif (a), Estrela Granite Complex (b) and Serra do Rabo plutons (c). Redrawn from Barbosa (2004), Barros *et al*. (2001) and Sardinha *et al*. (2006).

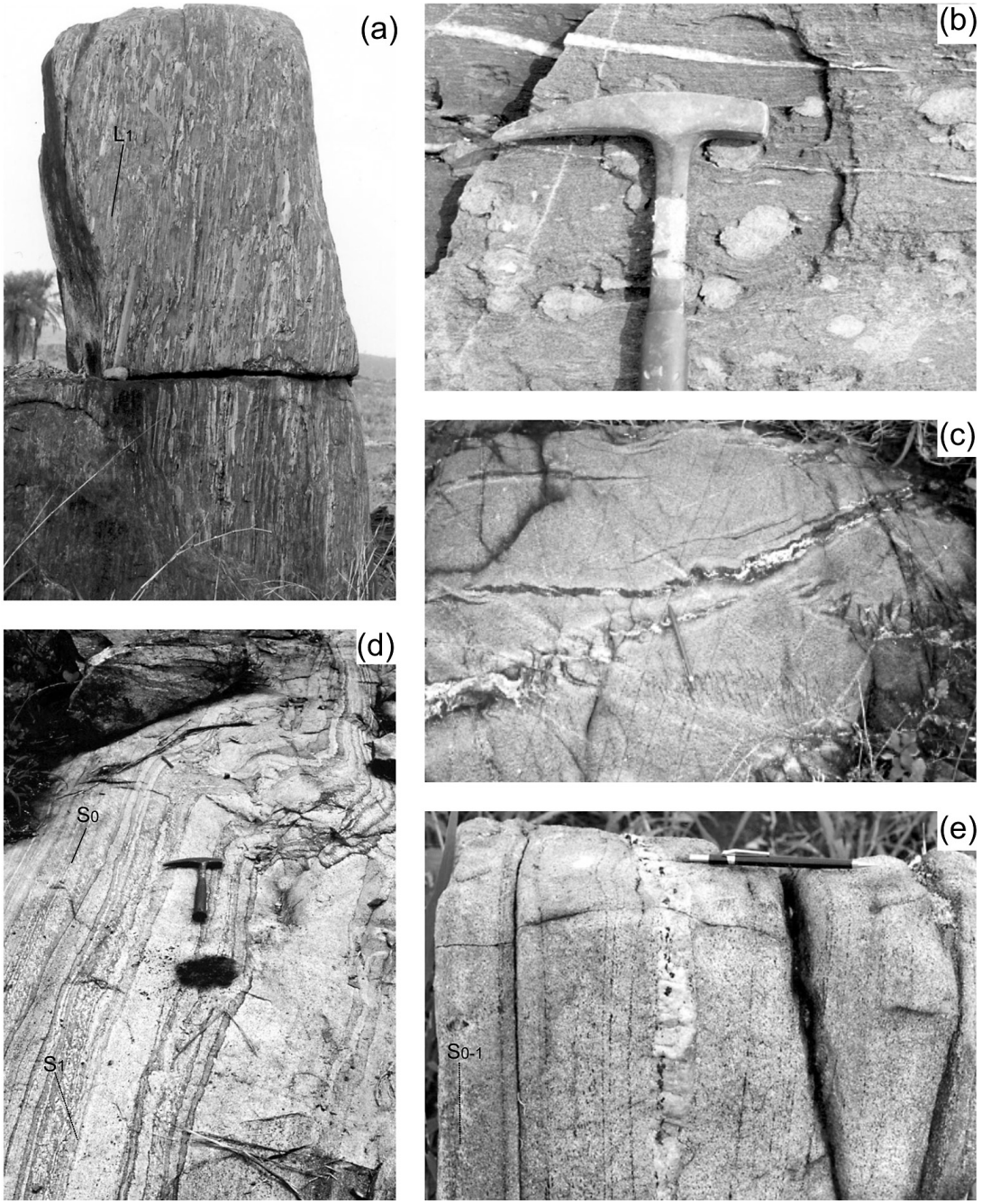

FIG. 3. The Estrela Granite Complex. (a) Host metabasic rocks from the inner aureole showing conspicuous subvertical stretching lineation (L_1). (b) Garnet porphyroblasts (light gray) in host metabasic rocks from the inner aureole south of the complex. (c) Conjugate *en échelon* amphibole- and plagioclase-bearing veins in a metabasic xenolith. (d) Flat-lying igneous layering in the core of the complex, cross-cut by a faint schistosity (S_1). (e) Subvertical composite foliation (S_0–S_1) in the eastern part of the complex.

solidus to low-temperature conditions. In contrast, the Serra do Rabo plutons show only a faint east–west-trending foliation (S_1) overprinted on non-layered rocks. Massive rocks occur in the southern pluton only.

The primary igneous layering in the Estrela and Igarapé Gelado massifs corresponds to rhythmically alternating ferromagnesian and quartzofeldspathic layers (Fig. 3d). Locally, conformable veins of aplite contribute to exaggerate this planar structure (Fig. 3e). In the center of the plutons, the layering is flat-lying, locally undulating or tightly folded, and overprinted by the east–west-trending S_1 foliation. It is steeply dipping in the periphery where it is indistinguishable from the foliation (composite S_0/S_1 surface). Therefore, the primary layering forms a dome structure.

The foliation (S_1) is outlined by the preferred orientation of ferromagnesian minerals, feldspars and ovoid quartz grains. It is generally penetrative at the scale

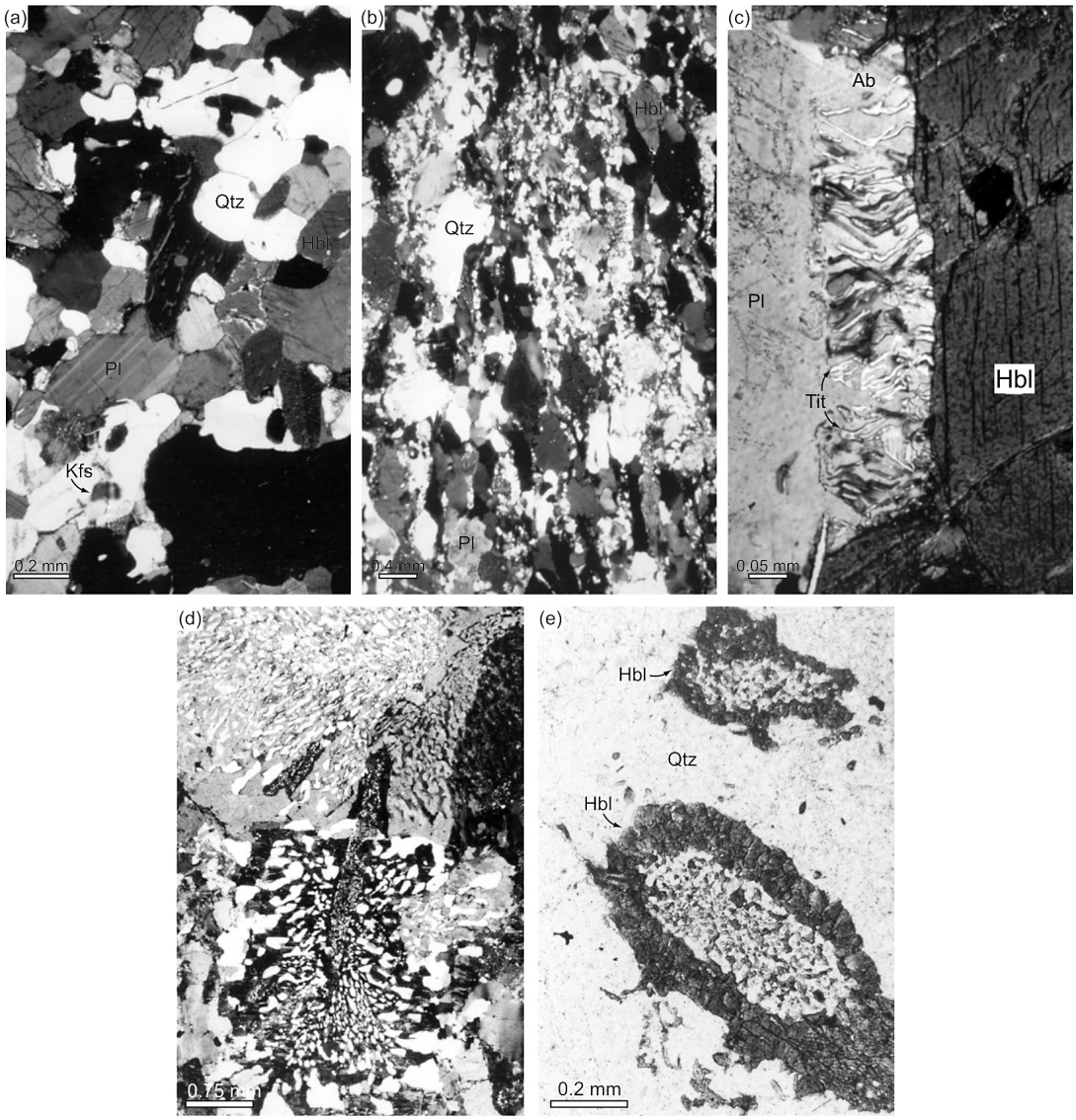

FIG. 4. Photomicrographs (cross-polarized light) showing (a) faint preferred orientation of minerals, (b) mylonitic foliation, (c) detail of albite–titanite symplectite developed at the expense of ferropargasite–hastingsite in relation with deformation, (d) a granophyric texture, and (e) sieve-textured amphibole. Photos a–c: Estrela granite complex; photos d–e: Serra do Rabo plutons.

of the bodies, but in some cases, it may be absent, as in some places in the Serra do Rabo plutons, where granites commonly display a massive structure. In the Estrela complex, the foliation is better developed near the margins. In the less deformed rocks, granular or weakly oriented granular textures are common (Fig. 4a). As the intensity of deformation increases, the preferred orientation becomes more intense. Preferentially oriented amphibole and annite crystals, in contact with feldspars, may be partially replaced by albite + oxides or albite + titanite symplectites (Fig. 4c). These are developed along faces disposed orthogonally to the direction of shortening. Feldspars may display kink bands and incipient dynamic recrystallization along margins (mantle-and-core texture). Ferropargasite–hastingsite and annite may occur as asymmetrical or symmetrical porphyroclasts from which recrystallization tails help to outline the foliation. Quartz occurs as elongate aggregates of subgrains and neoblasts.

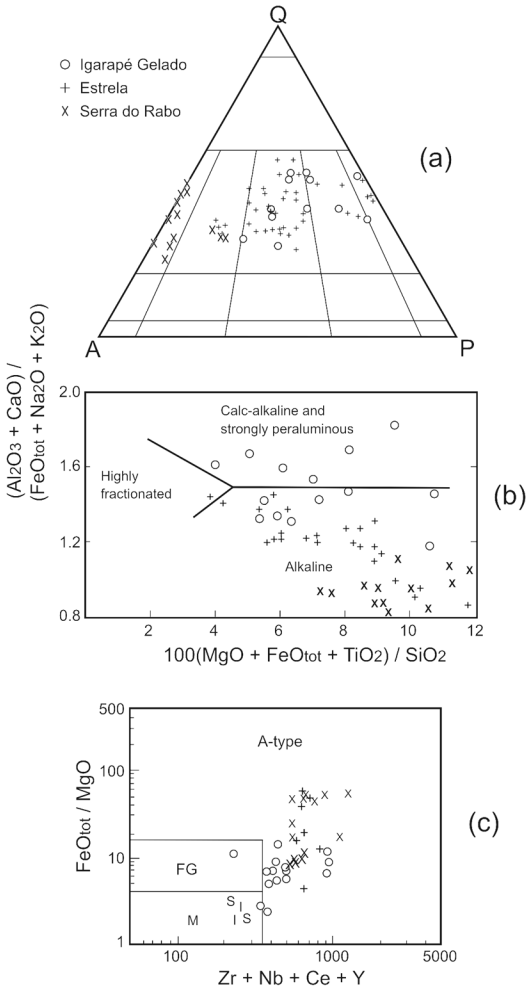

FIG. 5. Geochemical trends of the Carajás 2.7 Ga granites. (a) QAP diagram (Streckeisen 1976). (b) 100[(MgO + FeO_t + TiO_2)/SiO_2] *versus* (Al_2O_3 + CaO)/(FeO_t + Na_2O + K_2O) diagram (Sylvester 1989). (c) (FeO/MgO) *versus* (Zr + Nb + Ce + Y) diagram (Whalen *et al.* 1987).

Meter- to decimeter-wide mylonite zones (Fig. 4b) are generally conformable to the foliation (S_1). In places, relatively hot mylonites (~500°C) have been developed. Neoblasts of ferropargasite–hastingsite and feldspars compose the fine-grained matrix in these tectonites. Quartz grains consist of fine-grained neoblasts, which may occur obliquely to the mylonitic foliation. In some mylonite zones, ferropargasite–hastingsite crystals have been completely replaced by titanite. The stretching lineation is outlined by aggregates of neoblasts of quartz, feldspars and ferromagnesian phases, and show preferentially low dips. As these hot mylonites are found only within the batholiths and do not strike into the host metavolcanosedimentary rocks, they may be considered as the result of late mechanical adjustments during the emplacement history of the plutons, as discussed in the case of emplacement of synkinematic granites (Gapais 1989).

Low-temperature conjugate shear bands disposed broadly parallel to the foliation (S_1) occur locally in some of the massifs studied in the Carajás region. These shear bands are millimetric, and the symmetry of the array suggests coaxial deformation. Discrete dissolution-induced schistosity, outlined by dark insoluble material, can be observed in fine-grained rocks located near the margins of plutons.

PETROGRAPHY AND MINERALOGY

The Estrela granite complex and the Igarapé Gelado pluton consist of pinkish to whitish gray, fine- to medium-grained, locally porphyritic granites. The whitish varieties are in general the rocks having less modal annite and ferropargasite–hastingsite. In terms of facies variation, the two massifs present many similarities, monzogranites predominating largely over syenogranites, granodiorites and minor tonalites (Fig. 5a). The Serra do Rabo plutons consist of ferropargasite–hastingsite- and annite-bearing pink to pinkish gray alkali feldspar granites and syenogranites (Fig. 5a). Leucocratic rocks are also identified in these two plutons. The amounts of ferropargasite–hastingsite and annite are variable. Clinopyroxene is observed in a few cases. Sieve-textured amphibole occurs locally in rocks displaying a granophyric texture (Figs. 4d, e). In these cases, the core of amphibole grains contains small crystals of quartz, plagioclase and magnetite.

Rather abundant ferropargasite-bearing quartzo-feldspathic pegmatite and aplite veins cross-cut the granitic rocks of the three massifs. Early pegmatite veins are foliated and may show interlobate contacts with their host rocks, suggesting emplacement before

TABLE 1. SELECTED COMPOSITIONS OF AMPHIBOLE FROM THE ESTRELA GRANITE COMPLEX AND SERRA DO RABO PLUTONS

	Estrela granite complex							Serra do Rabo pluton			
Sample	VI62	VI62	CN22	CN22	CN24	CN24	CAP41	AC 43	AC 43	AC 47	AC 47
Anal.	18	28	41	52	32	33	21	2	12	30	31
SiO_2 wt%	39.41	39.34	37.62	37.13	37.45	37.06	37.51	37.11	40.24	36.94	36.97
Al_2O_3	9.27	9.56	10.99	10.80	10.45	10.83	10.63	12.50	10.50	12.50	12.40
TiO_2	1.55	1.14	1.54	1.32	1.19	1.11	1.03	0.36	0.97	0.09	0.08
FeO_{tot} *	31.65	33.01	32.75	31.46	31.56	32.17	32.49	30.21	29.65	32.51	32.46
MnO	0.18	0.10	0.31	0.32	0.08	0.15	0.4	0.32	0.29	0.58	0.53
MgO	1.23	1.16	0.81	0.72	1.38	1.38	0.44	2.37	2.70	0.18	0.28
CaO	10.50	10.35	10.26	10.68	10.69	10.80	10.6	10.62	10.63	10.60	10.63
Na_2O	1.74	1.68	1.92	1.66	1.79	1.43	1.78	1.48	1.28	1.31	1.36
K_2O	1.59	1.82	1.93	2.05	2.05	2.29	1.77	2.25	1.48	2.65	2.38
Total	97.12	98.29	98.13	96.14	96.77	97.34	96.65	97.20	97.70	97.39	97.08
Si *apfu*	6.119	6.415	6.162	6.192	6.197	6.086	6.228	6.014	6.435	6.086	6.091
^{IV}Al	1.696	1.585	1.838	1.808	1.803	1.914	1.772	1.986	1.565	1.914	1.909
^{VI}Al	0.000	0.252	0.283	0.315	0.235	0.183	0.309	0.401	0.414	0.513	0.499
Fe^{3+}	0.000	0.141	0.163	0.190	0.263	0.448	0.321	0.567	0.219	0.403	0.456
Ti	0.181	0.140	0.190	0.166	0.148	0.137	0.129	0.044	0.117	0.011	0.009
Fe^{2+}	4.353	4.361	4.323	4.198	4.106	3.950	4.210	3.528	3.746	4.076	4.016
Mn	0.024	0.014	0.043	0.045	0.011	0.021	0.056	0.0434	0.039	0.081	0.074
Mg	0.285	0.282	0.198	0.179	0.340	0.338	0.109	0.572	0.644	0.044	0.069
Ca	1.809	1.800	1.908	1.908	1.896	1.891	1.894	1.844	1.821	1.871	1.876
^{M4}Na	0.253	0.191	0.200	0.092	0.104	0.109	0.106	0.156	0.179	0.129	0.124
^{A}Na	0.271	0.339	0.410	0.445	0.470	0.356	0.459	0.309	0.218	0.290	0.311
K	0.315	0.379	0.403	0.436	0.433	0.480	0.375	0.465	0.302	0.557	0.500
Total	15.243	15.924	16.013	15.973	16.022	15.948	15.948	15.930	15.699	15.975	15.935
calc. FeO	31.650	31.976	31.561	30.100	29.667	28.896	30.188	26.029	28.012	29.585	29.15
calc. Fe_2O_3	0.000	1.149	1.321	1.511	2.104	3.639	2.558	4.647	1.820	3.251	3.679
*X*Fe	0.939	0.941	0.958	0.961	0.928	0.929	0.976	0.877	0.860	0.990	0.985

* Total iron expressed as FeO. The structural formula is calculated on the basis of 23 atoms of oxygen and 15 cations.

their complete consolidation. Tube-shaped megacrysts of ferropargasite are present locally in the pegmatite veins. The late veins are non-foliated (or weakly foliated in some cases) and have straight contacts with their host. Aplite also occur very commonly as stretched or boudinaged concordant veins or as folded veins.

Mineral compositions (Tables 1, 2) were determined using a Cameca SX50 electron microprobe (Laboratoire de Microanalyses, Université de Nancy) for the Estrela samples and a JEOL 8600 electron microprobe (Universidade de São Paulo) for the Serra do Rabo samples. The IMA-sanctioned nomenclature of Leake *et al.* (1997) and Rieder *et al.* (1998) was used to classify amphibole and biotite, respectively. In the Estrela granite complex, the mafic assemblage consists of ferropargasite and hastingsite (X_{Mg} in the range 0.01–0.21), annite (X_{Fe} in the range 0.86–0.97) and hedenbergite ($En_{17.9–19.7}$ $Fs_{32.0–35.2}Wo_{46.9–48.4}$). In tonalites, the Mg concentrations of the mafic mineral are higher (5.35–5.55% MgO). Plagioclase compositions vary from An_{11} to An_{23} in the various facies, but higher values ($An_{45–47}$) are observed in clinopyroxene–amphibole monzogranite. Microcline grains commonly contain microperthite and flame perthite. In the Serra do Rabo granites, the phase assemblage consists of hastingsite ($0.01 < X_{Mg} < 0.17$), ferropargasite ($0.02 < X_{Mg} < 0.20$), annite ($0.78 < X_{Fe} < 0.83$), oligoclase ($An_{10–15}$) and perthitic K-feldspar (flame perthite, mainly), which shows local replacement by chessboard albite.

Ilmenite is the main primary oxide phase in both massifs. It is locally replaced by titanite, forming a thin rind around grains. Magnetite is subordinate as a primary phase, but can occur as a deuteric product of destabilization of the primary mafic minerals. Other accessory minerals are zircon, allanite and apatite; they occur as euhedral crystals generally included in ferromagnesian phases or in plagioclase.

Whole-Rock Geochemistry

The samples from the Estrela granite complex were analyzed for major and trace elements by ICP–AES and ICP–MS (CRPG–CNRS, Vandoeuvre-lès-Nancy, France), whereas those from the Igarapé Gelado and

TABLE 2. SELECTED COMPOSITIONS OF BIOTITE FROM THE ESTRELA GRANITE COMPLEX AND SERRA DO RABO PLUTONS

	Estrela granite complex						Serra do Rabo pluton			
Sample	CRN33	CRN33	CAP41	VI62	CAP35	CN22	AC 43	AC 43	AC 43	AC 43
Anal.	41	54	22	20	40	51	39	43	47	46
SiO_2 wt%	33.89	32.98	32.72	33.90	33.27	33.06	34.55	34.60	34.52	34.27
Al_2O_3	14.49	14.33	13.58	12.68	13.70	12.60	14.13	14.68	14.44	14.58
TiO_2	1.71	1.46	3.20	4.28	2.94	3.93	1.90	1.71	1.73	1.79
FeO_{tot} *	33.13	34.32	35.46	35.02	33.02	35.39	30.44	29.57	29.89	30.44
MnO	0.28	0.17	0.29	0.02	0.14	0.23	0.20	0.24	0.20	0.20
MgO	2.68	3.17	0.61	1.41	3.06	1.01	3.62	3.86	3.91	3.76
CaO			0.01		0.05	0.05	0.06	0.05		
Na_2O	0.06	0.03	0.18	0.01	0.13	0.06	0.06	0.06	0.05	
K_2O	9.05	8.47	8.86	8.69	9.37	8.73	8.75	8.70	8.68	8.50
Total	95.37	95.02	94.90	96.16	95.54	95.19	93.69	93.47	93.49	93.64
Si *apfu*	5.572	5.473	5.499	5.577	5.483	5.536	5.688	5.678	5.674	5.637
^{IV}Al	2.428	2.527	2.501	2.423	2.517	2.464	2.312	2.322	2.326	2.363
^{VI}Al	0.380	0.276	0.189	0.035	0.144	0.022	0.430	0.517	0.473	0.463
Fe	4.555	4.763	4.984	4.818	4.551	4.956	4.190	4.058	4.109	4.187
Mg	0.657	0.784	0.153	0.346	0.752	0.015	0.888	0.944	0.958	0.921
Mn	0.039	0.024	0.041	0.003	0.020	0.252	0.028	0.033	0.028	0.028
Ti	0.211	0.182	0.404	0.529	0.364	0.033	0.235	0.211	0.214	0.221
Ca	0.000	0.000	0.000	0.000	0.002	0.000	0.008	0.009	0.011	0.009
Na	0.019	0.010	0.059	0.000	0.003	0.042	0.019	0.019	0.020	0.016
K	1.898	1.793	1.900	1.824	1.970	1.865	1.837	1.821	1.820	1.783
*X*Fe	0.874	0.859	0.970	0.933	0.858	0.952	0.825	0.811	0.811	0.820

* Total iron as Fe^{2+}. The structural formulae are calculated on the basis of 22 atoms of oxygen.

Serra do Rabo massifs were analyzed by X-ray fluorescence spectrometry and ICP–MS (Lakefield-Geosol laboratories, Belo Horizonte, Brazil).

The granite compositions (Table 3) are characterized by relatively high K_2O, Na_2O and FeO contents, low Al_2O_3 concentrations and high FeO/(FeO + MgO) values (0.83–0.99). The (K_2O + Na_2O)/CaO value increases from tonalites (1.37–1.81) to granodiorites (1.49–3.25) and monzogranites (2.41–8.00). The rocks are metaluminous to weakly peraluminous and subalkaline. On the basis of major elements, both the Serra do Rabo and the Estrela massifs show subalkaline affinities, whereas the Igarapé Gelado granites show an intermediate character. For example, in the diagram of Sylvester (1989), some samples plot in the alkaline field, whereas others plot in calc-alkaline field (Fig. 5b). In the Estrela granite complex, annite-rich monzogranites occurring preferentially in the center of the massif contain around 13.5 wt.% Al_2O_3, whereas ferropargasite-rich monzogranites found in the eastern domain of the complex have 11.5% Al_2O_3 (Table 3). In the Serra do Rabo granites, Al_2O_3 contents are between 10.1 and 13.1 wt.%. In the Igarapé Gelado pluton, granites have Al_2O_3 concentrations varying from 11.6 to 14.4 wt.%, though higher values are observed in some granodiorites (15.4%) and tonalites (16.0%).

The Estrela, Serra do Rabo and Igarapé Gelado granites show variable though generally high incompatible element contents (Table 3). The high values of Zr (146–713 ppm), Y (13–404 ppm), Nb (16–68 ppm), Ce (3–880 ppm), Rb (46–397) and Ga (21–30) are comparable to those of classic within-plate (Pearce *et al.* 1984) and A-type (Whalen *et al.* 1987) granites (Fig. 5c). Rare-earth elements (REE) patterns normalized to chondrite (Evensen *et al.* 1978) show high values, compared to orogenic granites. In the Estrela and Serra do Rabo massifs (Figs. 6a, c), the light REE are moderately fractionated [$3.04 < (La/Sm)_N < 7.78$], whereas heavy REE are only slightly fractionated [$1.04 < (Gd/Yb)_N < 1.78$]. Negative Eu anomalies are generally weak to moderate ($0.25 < Eu/Eu^* < 0.65$). Stronger negative Eu anomalies ($0.19 < Eu/Eu^* < 0.61$) are observed in a few samples of the Serra do Rabo plutons. In the Igarapé Gelado pluton (Fig. 6c), most samples show more pronounced fractionation (Fig. 6a) of both light and heavy REE [$4.34 < (La/Sm)_N < 38.93$; $1.03 < (Gd/Yb)_N < 7.51$], along with either variable negative ($0.30 < Eu/Eu^* < 0.99$) or slightly positive Eu anomalies ($1.07 < Eu/Eu^* < 1.74$). Therefore, the Igarapé Gelado massif shows geochemical traits intermediate between those of A-type metaluminous granites and high-K calc-alkaline granites.

Zircon Pb–Pb and U–Pb Geochronology

The granitic rocks from the Estrela, Igarapé Gelado and Serra do Rabo massifs have, in general, high modal proportions of prismatic crystals of zircon. In the first two massifs, zircon is commonly metamict, but relatively less altered grains can be found. On the contrary, the zircon crystals from the Serra do Rabo granites are abundant, well preserved, not fractured, and transparent, indicative of very slight metamictization.

Zircon grains have been dated in the Isotope Laboratory of the Universidade Federal do Pará. The Pb-evaporation method of Kober (1987) was applied to the Igarapé Gelado and Estrela granites (Tables 4, 5), whereas the U–Pb zircon method (Krogh 1973, Parrish *et al.* 1987, Mattison 1994) was used for the Serra do Rabo massif (Table 6). In the Pb-evaporation method, zircon grains are submitted to three heating steps (1450°, 1500°, 1550°C). Ages are then calculated through corrections for common Pb according to the double-stage evolution model (Stacey & Kramers 1975). In both methods, isotopic compositions were determined using a Finnigan Mat 262 mass spectrometer.

Zircon ages obtained by the two methods are 2763 ± 7 Ma for the Estrela granite complex, 2731 ± 26 Ma for the Igarapé Gelado massif and 2743 ± 1.6 Ma for one of the two Serra do Rabo plutons. These results show that the emplacement of A-type granites and the

TABLE 3. SELECTED WHOLE-ROCK COMPOSITIONS OF THE ARCHEAN A-TYPE GRANITES FROM CARAJÁS PROVINCE

	Igarapé Gelado massif			Estrela granite complex							Serra do Rabo pluton			
	Grd JP-45	Mzg JP-30	Mzg JP-47	Mzg CAP 14	Mzg CAP 39	Mzg CAP 43	Mzg CAP 13	Sy-gr CAP 35	Grd CAP 5	Ton CAP 40	Sy-gr	Gr	Gr	Gr
SiO_2 wt%	69.50	73.00	72.50	72.60	70.41	71.50	69.83	67.30	72.43	63.34	68.1	73.3	69.9	72.2
Al_2O_3	14.20	12.40	13.50	13.06	13.51	12.97	11.44	11.50	11.30	15.17	12.6	11.1	11.8	12.10
Fe_2O_3 tot	4.06	4.24	3.75	3.91	4.91	4.40	8.32	9.33	6.08	7.26	6.65	4.85	6.85	4.78
TiO_2	0.34	0.69	0.45	0.21	0.30	0.25	0.62	0.68	0.52	0.73	0.8	0.36	0.46	0.32
MnO	0.02	0.06	0.03	0.02	0.04	0.02	0.05	0.03	0.06	0.04	0.09	0.04	0.06	0.08
MgO	0.46	0.29	0.39	0.24	0.37	0.25	0.19	0.54	0.12	1.50	0.68	0.27	0.15	0
CaO	2.00	2.50	1.60	1.18	1.67	1.60	1.60	2.46	3.13	4.42	2.7	0.96	1.7	1.2
Na_2O	3.30	4.60	3.20	3.46	3.93	3.21	3.22	1.96	4.09	4.85	3.60	2.40	3.40	3.30
K_2O	3.20	1.60	4.60	4.21	3.63	4.68	3.46	5.20	1.59	1.72	3.30	4.70	4.30	5.00
P_2O_5	0.09	0.13	0.06	0.03	0.06	0.04	0.09	0.12	0.05	0.26	0.21	0.04	0.07	0.02
L.O.I	0.60	0.41	0.52	0.81	1.18	0.78	0.90	0.44	0.30	0.49	0.19	0.46	0.2	0.26
Total	97.77	99.92	100.60	99.73	100.01	99.70	99.72	99.56	99.67	99.78	98.92	98.48	98.89	99.26
Ba ppm	1756	575	895	758	685	915	650	1968	860	315	1574	1913	1743	<10
Rb	101	57	119	185	176	158	102	170	54	139	53	53	75	102
Sr	225	94	71	54	59	60	15	42	73	145	246	121	66	261
Th			125	222	161	19	25	40	29	<5	14	9	881	
Zr	310	673	303	292	425	351	555	625	632	437	364	337	598	<10
Nb	40	68	50	29	32	25	27	26	32	27	20	24	18	<5
Y	16	91	90	85	81	74	100	100	138	68	38	71	56	43
Ga	27	28	28	24	29	24	24	27	27	29	29	30	24	77
Sn			5	3	4	4	10	6	4	<5	<5	<5	27	
La	57	228	1253	197.7	281.5	213.6	70.0	79.2	138.2	56.2	49.6	56.5	58.5	502.1
Ce	18	143	723	320.6	440.9	351.9	143.4	158.1	281.9	115.1	95.3	115.2	118.7	880.6
Pr			32.9	44.6	33.6	16.7	17.8	32.9	13.6					
Nd	9	80	268	110.1	143.3	109.4	65.5	69.7	121.1	54.0	39.1	51.7	49.4	327.1
Sm	3	52	140	18.6	23.5	17.3	14.3	15.3	23.1	11.6	8.0	12.6	11.3	55.9
Eu	2	20	32	1.5	1.9	1.5	2.7	3.3	2.6	1.7	1.7	1.8	2.8	3.3
Gd	2	40	80	16.7	20.3	14.9	14.9	14.8	22.2	10.8	6.9	11.6	9.5	38.7
Tb			2.4	2.7	2.2	2.5	2.6	3.6	1.7					
Dy	2	25	39	14.1	14.3	12.7	16.1	16.4	22.8	10.7	5.6	11.0	6.8	23.0
Ho	1	18	26	3.1	2.8	2.7	3.7	3.8	5.0	2.4	1.1	2.1	1.1	4.4
Er	1	17	28	7.9	7.6	6.9	10.4	10.0	13.6	6.6	2.9	5.9	2.8	10.3
Tm			1.2	1.1	1.1	1.6	1.5	2.1	1.0					
Yb	2	14	18	7.8	7.1	6.8	10.6	10.6	14.7	7.2	2.5	5.2	1.9	8.0
Lu	2	8	17	1.2	1.1	1.0	1.6	1.6	2.1	1.1	0.4	0.8	0.3	1.3

Symbols: Sy-gr: syenogranite, Gr: granite, Mzg: monzogranite, Grd: granodiorite, Ton: tonalite.

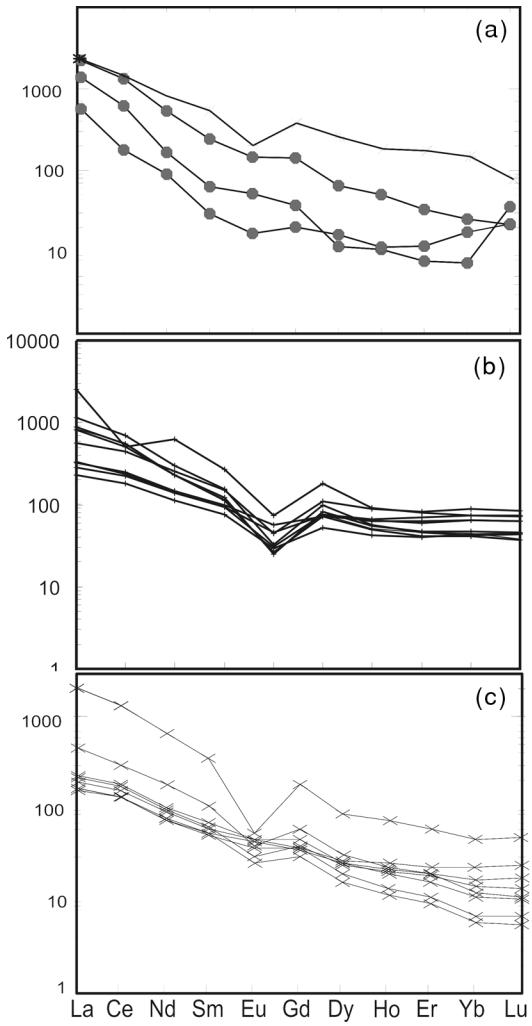

FIG. 6. Representative chondrite-normalized (Evensen *et al.* 1978) REE patterns for the Igarapé Gelado pluton (a), the Estrela granite complex (b) and the Serra do Rabo plutons (c).

related regional horizontal shortening event occurred during the late Archean times in the Carajás Province.

Sm–Nd Isotope Data

The Sm–Nd isotopic compositions (Table 7) were determined for the Estrela granite complex from monzogranites having variable amounts of ferromagnesian minerals: hedenbergite < ferropargasite (PSV–22), ferropargasite (PSV–75), annite < ferropargasite (PSV–62), ferropargasite < annite (CN–40) and annite (PSV–77). Sample preparation involved treatment with HF and HNO_3, followed by chemical separation in chromatography columns. Analyses were performed using a Finnigan Mat 262 mass spectrometer (Isotope Laboratory of the Universidade Federal do Pará) after deposition of Nd and Sm on filaments of Ta and Re, respectively. Similarly to the evaporation of Pb from zircon, the analyses of Sm and Nd were performed on a filament for evaporation and on another one for ionization.

Ratios measured of Nd isotopes were corrected for mass fractionation by use of $^{146}Nd/^{144}Nd = 0.7219$ as the parameter for normalization. Model ages were calculated from the depleted-mantle evolution curve (DePaolo 1981). The $^{147}Sm/^{144}Nd$ values (Table 7) range from 0.10221 to 0.12729. The $\varepsilon_{Nd(t)}$ values are slightly negative (–0.38 to –2.06), with model ages (T_{DM}) ranging from 2.97 to 3.19 Ga.

Discussion

The 2.7 Ga A-type granites and their coeval calc-alkaline counterparts record, in the Carajás region, an episode of weak and protracted horizontal shortening, most probably related to an active continental margin orogeny. High-temperature A-type magmas could have been produced under high thermal gradients as expected in Archean times. The high temperature and low viscosity of magmas would have led to rapid ascent of melts + crystals and to emplacement in a shallow-level volcanic sequence previously metamorphosed under greenschist-facies conditions. Low-pressure conditions of magma emplacement and crystallization promoted the separation of fluid phases, which produced several petrographic textures. Under these conditions, the formation of pegmatite veins, the breakdown of amphibole into quartz – magnetite – albite (Rutherford & Hill 1993), and the rapid crystallization of tube-shaped amphibole in pegmatites occurred, as well as granophyric intergrowths (Candela 1997). The presence of ilmenite as the main oxide phase and ferropargasite (Gilbert 1966), annite (Eugster & Wones 1962), and hedenbergite (Kurshakova & Avetisyan 1974) as the main mafic minerals points to the crystallization of magmas under conditions of relatively low fugacity of oxygen (~ magnetite–wüstite and wüstite–iron buffers).

The observed lithological variation seems to reflect recurrent injection of batches of magmas of variable composition rather than *in situ* fractional crystallization. Indeed, such a process cannot account for contrasted rocks present in the Estrela granite complex, such as hornblende monzogranites having 11.5% Al_2O_3 beside annite monzogranites displaying 13.5% Al_2O_3. Continuous filling of the magma chambers would have promoted lateral expansion (inflation) and consequently stronger flattening of the peripheral earlier pulses. The synkinematic emplacement of the 2.7 Ga A-type granites from the Carajás metallogenic province is indicated by the following criteria: (1) elongate shape

TABLE 4. ZIRCON Pb–Pb EVAPORATION DATA
FOR THE IGARAPÉ GELADO GRANITES, CARAJÁS PROVINCE

Zircon	T°C	Ratio	$^{204}Pb/^{206}Pb$	2σ	$^{208}Pb/^{206}Pb$	2σ	$^{207}Pb/^{206}Pb$	2σ	$(^{207}Pb/^{206}Pb)_c$	2σ	Age	2σ
JP10/1	1450	0/32	0.000181	4	0.11243	57	0.17098	27	0.16874	23	2545	2
	1500	0/36	0.000003	1	0.08380	47	0.17771	23	0.17767	23	2632	2
	1550	36/36	0.000005	2	0.07122	3	0.18106	45	0.18104	47	2663	4
JP10/2	1450	0/38	0.000028	3	0.05967	32	0.17096	2	0.17066	21	2565	2
	1500	0/34	0.000002	1	0.07425	3	0.17976	29	0.17975	27	2651	3
	1550	40/40	0.000000		0.13437	94	0.18661	23	0.18661	23	**2713**	2
JP10/3	1500	0/34	0.000000	0	0.08199	4	0.18622	21	0.18622	21	2709	2
	1550	8/8	0.000000	0	0.10365	51	0.18866	3	0.18866	3	**2731**	26
JP10/4	1500	0/32	0.000006	5	0.04154	29	0.17062	24	0.17060	24	2564	2
	1550	38/38	0.000002	4	0.04786	17	0.17888	28	0.17886	28	2643	3
JP10/5	1450	0/6	0.000000	0	0.05609	36	0.17313	49	0.17313	49	2588	5
	1500	8/8	0.000000	0	0.05604	144	0.18180	163	0.18180	163	2670	15
JP10/6	1500	0/28	0.000017	2	0.04560	42	0.16767	61	0.16749	65	2533	7
	1550	0/32	0.000007	6	0.05944	51	0.18208	34	0.18203	34	2672	3
	1580	34/34	0.000024	12	0.05803	39	0.18642	3	0.18639	31	**2711**	3
JP10/7	1500	0/30	0.000016	4	0.06159	45	0.17206	34	0.17186	29	2576	3
	1550	0/40	0.000005	2	0.10135	5	0.18156	4	0.18150	4	2667	4
	1580	0/38	0.000004	3	0.11806	57	0.18480	31	0.18477	33	2696	3
	1600	36/36	0.000014	2	0.12183	34	0.18652	38	0.18644	39	**2711**	3
JP10/8	1450	0/32	0.000020	3	0.04719	21	0.16970	29	0.16923	28	2550	3
	1500	0/36	0.000011	3	0.06660	33	0.18107	21	0.18092	22	2662	2
	1550	36/36	0.000016	2	0.08922	39	0.18524	25	0.18505	25	2699	2
JP10/9	1450	0/40	0.000017	2	0.07203	79	0.16530	148	0.16500	136	2508	14
	1500	0/38	0.000006	3	0.07907	61	0.18229	38	0.18221	4	2673	4
	1550	32/32	0.000005	2	0.12947	43	0.18694	22	0.18690	22	**2716**	2
JP10/10	1500	4/4	0.000000	0	0.07493	62	0.16903	41	0.16903	41	2548	4
JP10/11	1500	38/38	0.000056	7	0.05059	71	0.17282	31	0.17179	38	2576	4
JP10/12	1500	0/38	0.000021	5	0.05201	39	0.16832	25	0.16808	3	2539	3
	1550	0/32	0.000021	5	0.04632	23	0.17259	131	0.17167	78	2574	8
	1580	6/6	0.000000	0	0.04929	117	0.17764	377	0.17764	377	2631	35

TABLE 5. ZIRCON Pb–Pb EVAPORATION DATA
FOR THE ESTRELA GRANITE COMPLEX, CARAJÁS PROVINCE

Zircon	T(°C)	Ratio	$^{204}Pb/^{296}Pb$ ± 2σ	$^{207}Pb/^{206}Pb$ ± 2σ	$(^{207}Pb/^{206}Pb)_c$ ±2σ	Age (Ma) ±2σ
CRN-8/2	1500	90	0.000000 ± 0	0.19187 ± 25	0.19187 ± 25	2759 ± 2
CRN-8/5	1500	80	0.000003 ± 2	0.19171 ± 33	0.19169 ± 34	2757 ± 3
CRN-8/8	1450	82	0.000000 ± 0	0.19403 ± 57	0.19403 ± 57	2777 ± 5
CRN-8/8	1500	82	0.000002 ± 1	0.19333 ± 27	0.19332 ± 27	2771 ± 2
CRN-8/8	1550	52	0.000000 ± 0	0.19397 ± 44	0.19397 ± 44	2776 ± 4
CRN-8/9	1450	52	0.000002 ± 2	0.19138 ± 49	0.19134 ± 49	2754 ± 4
CRN-8/9	1500	90	0.000000 ± 0	0.19101 ± 35	0.19101 ± 35	2751 ± 3
	Σ ratio	528		Calculated age		2763 ± 7

of the massifs parallel to the regional structures, (2) parallelism between structures observed within the plutons and in the inner and outer aureoles, (3) presence of synkinematic porphyroblasts of garnet in the host metabasic rocks located near the contact with the granite, (4) progressive deformation first above the solidus and then under conditions of decreasing temperature, and (5) coexistence of early strongly foliated pegmatites with less deformed later ones. The emplacement of the small body oriented in the north–south direction, located in the north domain of the Estrela granite complex seems to have benefitted from space created in a tension gash during north–south regional shortening. Similar cases have been documented in the synkinematic Paleoproterozoic plutons emplaced in the West African craton (Pons *et al.* 1995).

The choice of an adequate petrogenetic model able to give rise to A-type magmas depends on the tectonic regimes during which the magmas were emplaced. In rift-related tectonics or stable terranes, A-type granites are considered to be produced by extensive fractionation of mantle-derived mafic magmas (Turner *et al.* 1992, Whalen *et al.* 1996). On the other hand, A-type granitic magmas emplaced during compressive stresses are

considered to originate by partial melting of continental sources (Sylvester 1989). The overall compressional regime during emplacement of 2.7 Ga A-type granites of the Carajás region and the absence of mafic magmas coeval with these granites (lack of mafic enclaves) seem to rule out a petrogenetic model invoking fractionation of mafic magma. A petrogenetic model involving partial melting of crustal sources, as proposed by several authors (Clemens *et al.* 1986, Creaser *et al.* 1991, Landenberger & Collins 1996, Skjerlie & Johnston 1993, Patiño-Douce 1997) seems to be applicable to the Archean A-type granites from the Carajás region. Indeed, the T_{DM} ages (2.96 to 3.01 Ga) obtained in the Estrela granite complex are very close to the ages of the older granulites occurring in the area, and dated by Pidgeon *et al.* (2000) at 3002 ± 14 Ma. Moreover, the high contents of incompatible elements observed in the A-type granites studied could have been promoted by high-temperature partial melting of anhydrous sources such as granulites (Clemens *et al.* 1896, Skjerlie & Johnston 1993, Landenberger & Collins 1996).

Alternative models of partial melting to produce A-type granites consider other crustal sources than granulites, such as tonalites and granodiorites (Anderson & Bender 1989, Patiño-Douce 1997). For the 2.7 Ga A-type granites from the Carajás region, such sources could be represented by 2.87 Ga calc-alkaline tonalites and sanukitoid granodiorites similar to those outcropping in the most southerly part of the Rio Maria domain (Althoff *et al.* 2000). Other areas of occurrence of 2.8 Ga calc-alkaline tonalites found to the northeast of the Estrela granite complex (Machado *et al.* 1991) suggest that these rocks could be more abundant than previously thought in the northern domain of the Carajás metallogenic province. These 2.8 Ga calc-alkaline granitic rocks could be good candidates as alternative source-rocks. This hypothesis needs to be tested in future on the basis of Sm–Nd isotopic data.

TABLE 6. U–Pb DATA FOR THE SERRA DO RABO GRANITES, CARAJÁS PROVINCE

Sample	Weight g	$^{206}Pb/^{204}Pb$	$^{206}Pb/^{204}Pb$ corr.	$^{207}Pb^*/^{235}U$ % error	$^{207}Pb^*/^{235}U$	$^{206}Pb^*/^{238}U$ % error	$^{206}Pb^*/^{238}U$
AC-30B1	0.00151	151.921	2631.79	0.61	132.062	0.218	0.506038
AC-30B2	0.00142	205.716	5922.37	0.518	123.936	0.184	0.477052
AC-30C	0.00145	893.067	1981.02	0.522	128.696	0.217	0.493952
AC-30D1	0.00094	885.498	1322.43	0.792	126.625	0.283	0.484626
AC-30E	0.00182	162.663	857.483	3.0	126.259	0.345	0.483791
AC-30M	0.00050	11.426	999.032	0.2	131.669	0.178	0.503969
AC-30I	0.00100	982.577	2326.54	0.522	140.913	0.223	0.537561

Sample	Rho % error	$^{207}Pb^*/^{206}Pb^*$ 6/8-7/5	$^{207}Pb^*/^{206}Pb^*$	$^{206}Pb^*/^{238}U$ % error	$^{207}Pb^*/^{235}U$ age, Ma	$^{207}Pb^*/^{206}Pb^*$ age, Ma	$^{207}Pb^*/^{206}Pb^*$ age, Ma
AC-30B1	0.214	0.979382	0.189275	0.0441	2639.7	2694.5	2735.87
AC-30B2	0.180	0.978679	0.188421	0.0378	2514.4	2634.69	2728.43
AC-30C	0.168	0.77701	0.188964	0.137	2587.8	2670.15	2733.17
AC-30D1	0.245	0.87205	0.189501	0.139	2547.4	2654.87	2737.83
AC-30E	0.186	0.70862	0.18928	0.25	2543.8	2652.16	2735.92
AC-30M	0.173	0.971952	0.189487	0.0418	2630.8	2691.69	2737.71
AC-30I	0.211	0.948116	0.190118	0.0707	2773.2	2755.87	2743.18

* Radiogenic isotopes. Pb corrected for common lead according to the Stacey & Kramers (1975) model for T = 2743 Ma.

TABLE 7. Sm–Nd DATA FOR THE ESTRELA GRANITE COMPLEX, CARAJÁS PROVINCE

Samples	Sm ppm	Nd ppm	$^{147}Sm/^{144}Nd$	2σ	$^{143}Nd/^{144}Nd$	2σ	$\varepsilon_{Nd(0)}$	$T_{(DM)}$ Ga	$\varepsilon_{Nd(t)}$
PSV-22	14.72	87.05	0.10221	0.00021	0.510853	0.000006	-34.82	3.03	-1.22
CN-40	11.67	67.97	0.10378	0.00054	0.510892	0.000032	-34.06	3.02	-1.02
PSV-77	5.85	33.67	0.10503	0.00042	0.510947	0.000016	-32.99	2.97	-0.38
PSV-62	16.17	76.89	0.12716	0.00048	0.511265	0.000027	-26.78	3.19	-2.06
PSV-75	16.04	76.20	0.12729	0.00144	0.511304	0.000036	-26.02	3.12	-1.34

Partial melting of slightly different sources, as proposed by Landenberger & Collins (1996), could explain the origin of coeval A-type and I-type granites in magmatic arcs. The differences in the rare-earth elements patterns of the Igarapé Gelado granites compared to those of the Estrela and Serra do Rabo granites could be tentatively explained by differences in depth of the source. The stronger fractionation of heavy rare-earth elements observed in the Igarapé Gelado granites suggest that the relevant magmas could have been produced at deeper levels of the crust, where garnet is expected to be a stable residual phase. Crustal thickening promoted by the compressive environment (magmatic arc or suture zone) in a context of high thermal gradients such as those expected in Archean times would be able to melt relatively anhydrous sources as granulites or mafic to intermediate meta-igneous rocks. In this view, the shallower sources would have led to the Estrela and Serra do Rabo granites, whereas deeper sources would have given rise to most of the Igarapé Gelado granites.

Conclusions

Lithochemical and mineralogical data indicate that the 2.7 Ga granitic rocks from the Carajás region are considered as metaluminous or weakly peraluminous A-type granites. The particular aspects of the granites discussed in this paper reside in their synkinematic emplacement, considered to be uncommon for granites of subalkaline affinities. The structural data indicate that they were emplaced synchronously with protracted horizontal shortening. The high temperature of the granitic magmas promoted rheological changes in the host rocks, producing a kilometer-wide aureole around the larger plutons. Ductile flattening of the aureole produced dome-and-keel patterns. The relatively high temperatures, considered to be necessary to give rise to the crust-derived A-type granites, would have been possible owing to the steep thermal gradients expected during Archean times. The various petrographic facies observed in plutons are interpreted to reflect differences in the composition of the pulses of magma. The rather hybrid chemical nature of the Igarapé Gelado granites could be explained by partial melting of sources located rather deeper in the crust compared to the possible sources of the coeval A-type granites.

Worthy of note is the similarity between the evolution of the Carajás metallogenic province and the history of other Archean provinces. Granite magmatism, deformation and metamorphism dated at *ca*. 2.7 Ga have been identified in the Superior Province of Canada (Beakhouse & McNutt 1991), in the Murchison Province and in the Norseman–Wiluna Belt, both from the Yilgarn craton (Hill *et al*. 1989, Witt & Swager 1989, Wiedenbeck & Watkins 1993). Even if the 2.7 Ga rocks from Canada are not chemically similar to those of the A-type granites studied from the Carajás region, one can conclude that granite generation related to both magmatic arcs and collision environments occurred at that time on a worldwide scale in response to soft amalgamation of hot continental microplates.

Acknowledgements

This work benefitted from financial and infrastructural support of the Universidade Federal do Pará (Centro de Geociências – PRONEX Program), Centre de Recherches Pétrographiques et Géologiques (CRPG–CNRS), Conselho Nacional de Desenvolvimento Científico e Tecnológico (CNPq), Coordenação de Aperfeiçoamento de Pessoal de Nível Superior (CAPES) and Companhia Vale do Rio Doce (CVRD). This paper is a contribution to the IGCP–510 project (IUGS – UNESCO). We thank the referees, Drs. Paul Sylvester and Reinhardt Fuck, and also the editor, Dr. Robert F. Martin, for valuable suggestions, comments and touchups to the text.

References

Almeida, F.F.M., Hasui, Y., Brito-Neves, B.B. & Fuck, R.A. (1981): Brazilian structural provinces: an introduction. *Earth Sci. Rev.* **17**, 1-29.

Althoff, F.J., Barbey, P. & Boullier, A.M. (2000): 2.8–3.0 Ga plutonism and deformation in the SE Amazonian craton: the Archean granitoids of Marajoara (Carajás Mineral Province, Brazil). *Precamb. Res.* **104**, 187-206.

Anderson, J.L. & Bender, E. (1989): Nature and origin of Proterozoic A-type granitic magmatism in the southwestern United States of America. *Lithos* **23**, 19-52.

Anderson, J.L. & Smith D.R. (1995): The effects of temperature and fO_2 on the Al-in-hornblende barometer. *Am. Mineral.* **80**, 549-559.

Arzi, A.A. (1978): Critical phenomena in the rheology of partially melted rocks. *Tectonophysics* **44**, 173-184.

Barbosa, J.P.O. (2004): *Geologia Estrutural, Geoquímica, Petrografia e Geocronologia de granitóides da região de Igarapé Gelado, norte da Província Mineral de Carajás*. Master's thesis, Universidade Federal do Pará, Belém, Brazil.

Barros, C.E.M. & Barbey, P. (1998): A importância da granitogênese tardi-arqueana (2.5 Ga) na evolução tectono-metamórfica da província mineral de Carajás – o Complexo Granítico Estrela e sua auréola de contato. *Rev. Bras. Geoc.* **28**, 513-532.

Barros, C.E.M., Barbey, P. & Boullier, A.M. (2001): Role of magma pressure, tectonic stress and crystallization progress in the emplacement of the syntectonic granites. The A-type Estrela Granite Complex (Carajás Mineral Province, Brazil). *Tectonophysics* **343**, 93-109.

BARROS, C.E.M., DALL'AGNOL, R., BARBEY, P. & BOULLIER, A.M. (1997): Geochemistry of the Estrela granite complex, Carajás region, Brazil: an example of an Archaean A-type granitoid. *J. South Am. Earth Sci.* **10**, 321-330.

BARROS, C.E.M., DALL'AGNOL, R., SOARES, A.D.V. & DIAS, G.S. (1994): Metagabros de Águas Claras, Serra dos Carajás: petrografia, geoquímica e transformações metamórfico-hidrotermais. *Acta Geol. Leopold.* **40**, 1-70.

BEAKHOUSE, G.P. & MCNUTT, R.H. (1991): Contrasting types of Late Archean plutonic rocks in northeastern Ontario: implications for crustal evolution in the Superior Province. *Precamb. Res.* **49**, 141-165.

BETTENCOURT, J.S., LEITE, W.B., Jr., GORAIEB, C.L., SPARRENBERGER, I., BELLO, R.M.S. & PAYOLLA, B.L. (2005): Sn–polymetallic greisen-type deposits associated with late-stage rapakivi granites, Brazil: fluid inclusion and stable isotope characteristics. *Lithos* **80**, 363-386.

BRUN, J.P. & PONS, J. (1981): Strain patterns of pluton emplacement in a crust undergoing non-coaxial deformation, Sierra Morena, southern Spain. *J. Struct. Geol.* **3**, 219-229.

CANDELA, P.A. (1997): A review of shallow, ore-related granites: textures, volatiles, and ore metals. *J. Petrol.* **38**, 1619-1633.

CLEMENS, J.D., HOLLOWAY, J.R. & WHITE, A.J.R. (1986): Origin of an A-type granite: experimental constraints. *Am. Mineral.* **71**, 317-324.

COSTI, H.T., DALL'AGNOL, R., BORGES, R.M.K., MINUZZI, O.R.R. & TEIXEIRA, J.T. (2002): Tin-bearing sodic epysienites associated with the Proterozoic, A-type Água Boa granite, Pitinga mine, Amazonian craton, Brazil. *Gondwana Res.* **5**, 435-451.

CREASER, R.A., PRICE, R.C. & WORMALD, R.J. (1991): A-type granites revisited: assessment of a residual-source model. *Geology* **19**, 163-166.

DALL'AGNOL, R., SOUZA, Z.S., ALTHOFF, F.J., BARROS, C.E.M., LEITE, A.A.S. & JORGE-JOÃO, X.S. (1997): General aspects of the granitogenesis of the Carajás Metalogenic Province. *In* Int. Symp. on Granites and Associated Mineralizations, Excursion Guide, CBPM, ISGAM, 2 (Salvador), 135-161.

DALL'AGNOL, R., TEIXEIRA, N.P., RÄMÖ, O.T., MOURA, C.A.V., MACAMBIRA, M.J.B. & OLIVEIRA, D.C. (2005): Petrogenesis of the Paleoproterozoic rapakivi A-type granites of the Archean Carajás metallogenic province, Brazil. *Lithos* **80**, 101-129.

DEPAOLO, D.J. (1981): Nd isotopic studies: some new perspectives on Earth structure and evolution. *Trans. Am. Geophys. Union* (*EOS*), 137-140.

DOCEGEO (Rio Doce Geologia e Mineração) (1988): Revisão litoestratigráfica da Província Mineral de Carajás. *In* Província Mineral de Carajás, Litoestratigrafia e principais depósitos minerais. CVRD/SBG, *Congr. Bras. Geol.*, (Belém), *Anexo aos anais* **35**, 11-59.

EBY, G.N. (1992): Chemical subdivision of the A-type granitoids: petrogenetic and tectonic implications. *Geology* **20**, 641-644.

EUGSTER, H.P. & WONES, D.R. (1962): Stability relations of the ferruginous biotite, annite. *J. Petrol.* **3**, 82-125.

EVENSEN, N.M., HAMILTON, P.J. & O'NIONS, R.K. (1978): Rare-earth abundances in chondritic meteorites. *Geochim. Cosmochim. Acta* **42**, 1199-1212.

GAPAIS, D. (1989): *Les orthogneiss: structures, mécanismes de déformation et analyse cinématique*. *Mém. Doc. Centre Armoricain Et. Struct. Socles* (*Rennes*) **28**.

GILBERT, M.C. (1966): Synthesis and stability relations of the hornblende ferropargasite. *Am. J. Sci.* **264**, 698-742.

GIRET, A., BONIN, B. & LÉGER, J.M. (1980): Amphibole compositional trends in oversaturated and undersaturated alkaline plutonic ring-complexes. *Can. Mineral.* **18**, 491-495.

HAAPALA, I. (1995): Metallogeny of the rapakivi granites. *Mineral. Petrol.* **54**, 149-160.

HILL, R.I., CAMPBELL, I.H. & COMPSTON, W. (1989): Age and origin of granitic rocks in the Kalgoorlie–Norseman region of Western Australia: implications for the origin of Archaean crust. *Geochim. Cosmochim. Acta* **53**, 1259-1275.

HUHN, S.R.B., MACAMBIRA, M.J.B. & DALL'AGNOL, R. (1999): Geologia e Geocronologia Pb/Pb do granito alcalino Arqueano Planalto, Região da Serra do Rabo, Carajás – PA. *Simp. Geol. Amazônia, 6, Manaus, Anais* **1**, 463-466.

KOBER, B. (1987): Single-zircon evaporation combined with Pb^+ emitter bedding $^{207}Pb/^{206}Pb$-age investigations using thermal ion mass spectrometry, and implications to zirconology. *Contrib. Mineral. Petrol.* **96**, 63-71.

KROGH, T.E. (1973): A low contamination method for hydrothermal decomposition of zircon and extraction of U and Pb for isotopic age determinations. *Geochim. Cosmochim. Acta* **37**, 485-494.

KURSHAKOVA, L.D. & AVETISYAN, E.I. (1974): Stability and properties of synthetic hedenbergite. *Geochim. Int.* **3**, 338-346.

LANDENBERGER, B. & COLLINS, W.J. (1996): Derivation of A-type granites from a dehydrated charnockitic lower crust: evidence from a Chaelundi Complex, eastern Australia. *J. Petrol.* **37**, 145-170.

LEAKE, B.E., WOOLLEY, A.R., ARPS, C.E.S., BIRCH, W.D., GILBERT, M.C., GRICE, J.D., HAWTHORNE, F.C., KATO, A., KISCH, H.J., KRIVOVICHEV, V.G., LINTHOUT, K., LAIRD, J., MANDARINO, J., MARESCH, W.V., NICKEL, E.H., ROCK, N.M.S., SCHUMACHER, J.C., SMITH, D.C., STEPHENSON,

N.C.N., UNGARETI, L., WHITTAKER, E.J.W. & GUO, YOUZHI (1997): Nomenclature of amphiboles. Report of the Subcommittee on Amphiboles of the International Mineralogical Association, Commission on New Minerals and Mineral Names. *Can. Mineral.* **35**, 219-246.

LEITE, A.A.S., DALL'AGNOL, R., MACAMBIRA, M.J.B. & ALTHOFF, F.J. (2004): Geologia e geocronologia dos granitóides arqueanos da região de Xinguara-PA e suas implicações na evolução do terreno granito-greenstone de Rio Maria, Cráton Amazônico. *Rev. Bras. Geoc.* **34**, 447-458.

LIVERTON, T. (1999): Highly evolved tin granites: a Canadian example. *Rev. Bras. Geoc.* **29**, 9-16.

LOISELLE, M.C. & WONES, D.R. (1979): Characteristics and origin of anorogenic granites. *Geol. Soc. Am., Abstr. Programs* **11**, 468.

MACHADO, N., LINDENMAYER, Z., KROGH, T.H. & LINDENMAYER, D. (1991): U–Pb geochronology of Archaean magmatism and basement reactivation in the Carajás area, Amazon shield, Brazil. *Precamb. Res.* **49**, 329-354.

MARTIN, R.F. (2006): A-type granites of crustal origin ultimately result from open-system fenitization-type reactions in an extensional environment. *Lithos* **91**, 125-136.

MATTISON, J.M. (1994): A study of complex discordance in zircons using step-wise dissolution techniques. *Contrib. Mineral. Petrol.* **116**, 117-129.

MILLER, R.B. & PATERSON, S.R. (1994): The transition from magmatic to high-temperature solid-state deformation: implications from the Mount Stuart Batholith, Washington. *J. Struct. Geol.* **16**, 853-865.

PARRISH, R.R., RODDICK, J.C., LOVERIDGE, W.D. & SULLIVAN, R.W. (1987): Uranium–lead analytical techniques at the geochronology laboratory, Geological Survey of Canada. *In* Radiogenic Age and Isotopic Studies: Report 1. *Geol. Surv. Can., Pap.* **87**, 3-7.

PATIÑO-DOUCE, A.E. (1997): Generation of metaluminous A-type granites by low-pressure melting of calc-alkaline granitoids. *Geology* **25**, 743-746.

PAWLEY, M.J. & COLLINS, W.J. (2002): The development of contrasting structures during the cooling and crystallization of a syn-kinematic pluton. *J. Struct. Geol.* **24**, 469-483.

PEARCE, J.A., HARRIS, N.B.W. & TINDLE, A.G. (1984): Trace element discrimination diagrams for the tectonic interpretation of granitic rocks. *J. Petrol.* **25**, 956-983.

PIDGEON, R.T., MACAMBIRA, M.J.B. & LAFON, J.-M. (2000): Th–U–Pb isotopic systems and internal structures of complex zircons from an enderbite from the Pium Complex, Carajás Province, Brazil: evidence for the ages of granulite facies metamorphism and the protolith of the enderbite. *Chem. Geol.* **166**, 159-171.

PINHEIRO, R.V.L. & HOLDSWORTH, R.E. (1997): Reactivation of Archaean strike–slip fault systems, Amazon region, Brazil. *J. Geol. Soc. London* **154**, 99-103.

PONS, J., BARBEY, P., DUPUIS, D. & LÉGER, J.M. (1995): Mechanisms of pluton emplacement and structural evolution of 2.1 Ga juvenile continental crust: the Birimian of south-western Niger. *Precamb. Res.* **70**, 281-301.

RÄMÖ, O.T., ed. (2005): Granitic systems – a special issue in honor of Ilmari Haapala. *Lithos* **80**, xi-xix.

RÄMÖ, O.T., DALL'AGNOL, R., MACAMBIRA, M.J.B., LEITE, A.A.S., OLIVEIRA, D.C. (2002): 1.88 Ga oxidized A-type granites of the Rio Maria region, eastern Amazonian craton: positively anorogenic! *J. Geol.* **110**, 603-610.

RIEDER, M., CAVAZZINI, G., D'YAKONOV, Y.S., FRANK-KAMENETSKII, V.A., GOTTARDI, G., GUGGENHEIM, S., KOVAL, P.V., MÜLLER, G., NEIVA, A.M.R., RADOSLOVICH, E.W., ROBERT J.L., SASSI, F.P., TAKEDA, H., WEISS, Z. & WONES, D.R. (1998): Nomenclature of the micas. *Can. Mineral.* **36**, 905-912.

RUTHERFORD, M.C. & HILL, P.M. (1993): Magma ascent rates from amphibole breakdown: an experimental study applied to the 1980–1986 Mount St. Helens eruptions. *J. Geophys. Res.* **98**, 19667-19685.

SARDINHA, A.S., BARROS, C.E.M. & KRYMSKY, R. (2006): Geology, geochemistry and U–Pb geochronology of the Archean (2.74 Ga) Serra do Rabo granite stocks, Carajás Metallogenic Province, northern Brazil. *J. S. Am. Earth Sci.* **20**, 327-339.

SKJERLIE, K.P. & JOHNSTON, A.D. (1993): Fluid-absent melting behavior of an F-rich tonalitic gneiss at mid-crustal pressures: implications for the generation of anorogenic granites. *J. Petrol.* **34**, 785-815.

STACEY, J.S. & KRAMERS, J.D. (1975): Approximation of terrestrial lead isotope evolution by a two-stage model. *Earth Planet. Sci. Lett.* **26**, 207-221.

STRECKEISEN, A. (1976): To each plutonic rock its proper name. *Earth Sci. Rev.* **12**, 1-33.

SYLVESTER, P.J. (1989): Post-collisional alkaline granites. *J. Geol.* **97**, 261-280.

SYLVESTER, P.J. (1994): Archean granite plutons. *In* Archean Crustal Evolution (K.C. Condie, ed.). Elsevier, Amsterdam, The Netherlands (261-314).

TASSINARI, C.C.G. & MACAMBIRA, M.J.B. (2004): A evolução tectônica do Cráton Amazônico. *In* O desvendar de um continente: a moderna geologia da América do Sul e o legado da obra de Fernando Flávio Marques de Almeida (V. Mantesso Neto, A. Bartorelli C.D.R. Carneiro & B.B.B. Neves, eds.). Beca, São Paulo, Brazil (471-486).

THOMPSON, A.G. & BARNES, C.G. (1999): 1.4-Ga peraluminous granites in central New Mexico Petrology and geo-

chemistry of the Priest pluton. *Rocky Mountain Geology* **34**, 223-243.

TURNER, S.P., FODEN, J.D. & MORRISON, R.S. (1992): Derivation of some A-type magmas by fractionation of basaltic magma: an example from the Padthaway Ridge, South Australia. *Lithos* **28**, 151-179.

VIGNERESSE, J.-L. (2004): A new paradigm for granite generation. *Trans. R. Soc. Edinburgh: Earth Sci.* **95**, 11-22.

VIGNERESSE, J.-L., BARBEY, P. & CUNEY, M. (1996): Rheological transitions during partial melting and crystallization with application to felsic magma segregation and transfer. *J. Petrol.* **37**, 1579-1600.

VIGNERESSE, J.-L. & CLEMENS, J.D. (2000): Granitic magma ascent and emplacement: neither diapirism nor neutral buoyancy. *In* From the Arctic to the Mediterranean: Salt, Shale and Igneous Diapirs in and around Europe (B. Vendeville, Y. Mart & J.-L. Vigneresse, eds.). *Geol. Soc., Spec. Publ.* **174**, 1-19.

WHALEN, J.B., CURRIE, K.L. & CHAPPELL, B.W. (1987): A-type granites: geochemical characteristics, discrimination and petrogenesis. *Contrib. Mineral. Petrol.* **95**, 407-419.

WHALEN, J.B., JENNER, G.A., LONGSTAFFE, F.J., ROBERT, F. & GARIÉPY, C. (1996): Geochemical and isotopic (O, Nd, Pb and Sr) constraints on A-type granite petrogenesis based on the Topsails Igneous Suite, Newfoundland Appalachians. *J. Petrol.* **37**, 1463-1489.

WIEDENBECK, M. & WATKINS, K.P. (1993): A time scale for granitoid emplacement in the Archean Murchinson Province, Western Australia, by single zircon geochronology. *Precamb. Res.* **61**, 1-26.

WITT, W.K. & SWAGER, C.P. (1989): Structural setting and geochemistry of Archaean I-type granites in the Bardoc–Coolgardie area of the Norseman–Wiluna Belt, Western Australia. *Precamb. Res.* **44**, 323-351.

Received November 20, 2007, revised manuscript accepted November 11, 2009.